Materials Research. 2014; 17(3): 638-649
DOI: http://dx.doi.org/10.1590/S1516-14392014005000030

Cartilage Reconstruction Using Self-anchoring Implant with Functional Gradient

***Karen Cristina Laurenti*[a], *Lourdes Cristina de Albuquerque Haach*[a],**

***Arnaldo Rodrigues dos Santos Jr.*[b], *João Manuel Domingos de Almeida Rollo*[c],**

***Rodrigo Bezerra de Menezes Reiff*[d], *Ana Maria Minarelli Gaspar*[e],**

Benedito de Moraes Purquerio*[a], *Carlos Alberto Fortulan*[a]

[a]*Departament of Mechanical Engineering, University of São Paulo – USP, Av. Trabalhador São Carlense, 400, CEP 13566-590, São Carlos, SP, Brazil*
[b]*Center for Natural Sciences and Humanities, University of ABC, Av. dos Estados, 5001, CEP 09210-971, Santo André, SP, Brazil*
[c]*Bioengineering Interunits, University of São Paulo – USP, Av. Trabalhador São Carlense, 400, CEP 13566-590, São Carlos, SP, Brazil*
[d]*Federal University of São Carlos – UFSCar, Rod. Washington Luís, Km 235, CEP 13565-905, São Carlos, SP, Brazil*
[e]*Laboratory of Morfology, Universidade Estadual Paulista Júlio de Mesquita – UNESP, Rua Humaitá, 1680, CEP 14801-903, Araraquara, São Paulo, SP, Brazil*

Received: July 16, 2013; Revised: February 10, 2014

This study presents an innovative and original biomaterial designed to substitute for articular cartilage and mimic its mechanical behavior, including elastic cushioning and the characteristics of fiber-reinforced gel. The material was composed of polyurethane and bioglass microfiber 45S5. It was designed to present a tribological surface to the cartilage of the tibial plateau, and to convert over a functional gradient to an osteointegrable region for self-anchorage to the subchondral bone. The biomaterial samples showed no toxicity and promoted cell spreading. Subsequent *in vivo* studies in rabbits demonstrated the formation of a rigid structure similar to bone trabeculae in the distal region of the tribological surface of the implant. The tribological surface of the proximal region showed a fibrocartilaginous tissue with highly vascularized chondrocytes, thus validating the proposed concept for the design of the implant incorporating a functional gradient and auto-stability.

Keywords: *osteochondral defect, polyurethane, microfiber 45S5 bioglass, cartilage repair, functional gradient*

1. Introduction

Articular cartilage is a highly resilient connective tissue covering the bone joint surfaces. In typical synovial joints, articular cartilage is a tribological and lubricated surface that promotes movement without considerable friction. This type of cartilage is hyaline and is mainly composed of chondrocytes surrounded by extracellular matrix[1,2]. The biomechanical properties of articular cartilage depend largely on the composition and integrity of the extracellular matrix. Because it is an avascular tissue, articular cartilage has a low regeneration capacity. Consequently, the cartilage lesions are healed by the formation of scar tissue composed mostly of fibrocartilage, which has weaker mechanical and biological properties than the original hyaline cartilage and which gradually degenerates over time, resulting in permanent loss of structure and function and leading to severe pain[1,3,4].

The degenerated cartilage can lead to either temporary or permanent physical disability and can be a result of a number of conditions, such as microorganisms (tuberculosis, syphilis), injuries secondary to inflammatory rheumatic diseases, traumatic injuries, and metabolic diseases[5].

The phenomenon of tissue healing can be divided into four natural phases: hemostasis, inflammation, proliferation, and remodeling. An injury restricted to the superficial layers of cartilage (chondral defect) does not entirely satisfy these three phases due to the avascular nature of the hyaline cartilage. On the other hand, when there is an osteochondral defect with exposure of the subchondral bone, all three stages occur naturally[6].

In most clinical situations, the joint itself can repair damage that does not disturb the integrity of the articular surface. A mechanical disruption of the surface cartilage stimulates chondral synthesis, but rarely results in injury repair. In turn, although bone and chondral repair can be induced by osteochondral lesions, the repaired tissue does not have the same mechanical and biological properties as the original cartilage[7]. Treatments to reconstitute damaged articular cartilage such as drilling, subchondral

*e-mail: cfortula@sc.usp.br

bone microfracture, and abrasion arthroplasty promote the formation of fibrous cartilage with different properties than those of the original hyaline tissue and therefore produce repairs of limited duration[8].

Focal lesions of the articular cartilage require surgical treatment ranging from classical methods for bone marrow stimulation such as debridement, multiple perforations, abrasions, and microfractures, to modern biological methods like pericondral and periosteal transplantation, autologous implantation of cultured chondrocyte, osteochondral autologous grafts[6,9], and more recently, to the use of biomaterials.

Among all the biomaterials used for tissue engineering, polyurethane has a structure that allows products with a wide range of physical and mechanical properties to be produced, making it suitable for use in a variety of applications, such as soft tissue and cartilage reconstruction and bone regeneration[10]. In technical applications, the polyurethane is applied as a coating following abrasion in water environment. Recent applications of biomaterials for tissue engineering have focused on the interaction with surrounding tissues[11], improving bioactivity by incorporating fillings or coatings of porous bioceramics on polymeric matrices[12].

Bioactive glass is an example of a biomaterial that causes a specific biological response *in vivo*, resulting in the formation of a strong bond between the living tissue (e.g. bone) and the biomaterial[13]. 45S5 bioglass is a important bioactive glass composed of SiO_2, Na_2O, CaO, and P_2O_5[13,14]. The main advantage of bioglass is the ability to unite both hard and soft tissues, since its bioactivity index is greater than 8. Moreover, it has been shown that the dissolution product of bioglass stimulates gene expression in osteoblasts[11] as well as angiogenesis[15]; thus, bioglass has been considered a material of choice for the development of bioactive composites for bone engineering[14].

For cartilage implants to be successful, it will be necessary to solve challenges associated with mechanical loading properties, friction/lubrication, mechanical anchorage, durability, and interaction with surrounding cartilage. To that end, this study describes a conceptually new implant and application to repair osteochondral defects in knees of rabbits. The sample was a cylindrical model composed of polyurethane, bioglass microfiber, and variations in porosity, designed as a biological structural and functional gradient material (FGM).

2. Material Methods

2.1. *Implant concept*

An implant with functionally graded characteristics, once deployed, must establish a compromise between mechanical properties and biocompatibility. In order to achieve this goal, implants composed of bioglass microfiber and porous polyurethane were produced using available and reproducible manufacturing techniques. The upper side of the implant is responsible for the mechanical characteristics, gradually shifting to the lower side, which permits mechanical fixation by osteointegration in the osteochondral region, as shown in Figure 1. Therefore, this design of composite material has the characteristics of a possible replacement for articular cartilage.

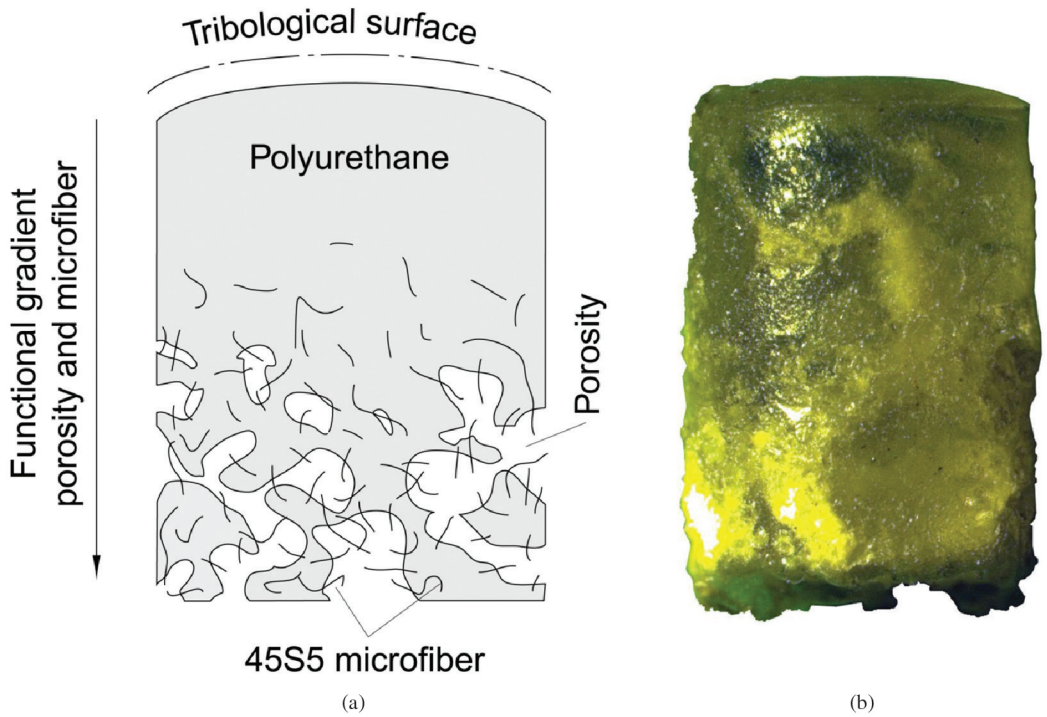

Figure 1. Implant of bioglass microfiber and polyurethane: a) schematic drawing; b) actual implant.

The processing methods and materials used were selected in order to meet the desired characteristics for the implant components, i.e., dimensional accuracy, mechanical reliability, service performance, repeatability, and acceptable cost. As a result, a structural material was obtained in functional gradient. The bioglass microfiber confers mechanical strength, rigidity, and adherence to biological tissue, while the polyurethane is responsible for the elastic-plastic behavior. This implant, when applied *in vivo,* is expected to maintain both the necessary mechanical properties and tribological characteristics (Figure 2). The overall dimensions of the samples for implantation were 3.0 mm diameter by 4.0 mm height. The aim is to design a material with new properties and functions that are impossible to find in a conventional homogeneous material.

2.2. *Materials*

The new material was developed using medical polyurethane (Tecothane® TPU TT-1074A, manufactured by Lubrizol® Advanced Materials Inc.) as a matrix and bioglass microfiber (manufactured by Mo-Sci Corporation) as a reinforcing and bone-integrating agent. TT-1074A has aromatic properties, a hardness of 75A-77D, a specific gravity of 1.1 g/cm^3, a tensile strength of 41 MPa, radiopacity, a normal color, and a melt processing temperature ranging from 190 °C to 220 °C. Mo-Sci bioglass microfiber has a specific gravity of 2.7 g/cm^3, an elastic modulus of 30 to 35 GPa, a tensile strength of 40 to 60 MPa, a refractive index of 1.55, a softening temperature of 550 °C, a dissolution rate of ~ 150 mg/cm^2/day, and thermal expansion of 16×10^{-6} cm/cm/°C. The following are typical chemical compositions: 45% SiO_2, 24.5% Na_2O, 6% P_2O_5. 300 µm diameter NaCl particles were used as a porogenic agent. After the implants were formed, they were leached with distilled water to remove NaCl, and were dried in vacuum desiccators over a 24-hour period.

2.3. *Manufacturing the implants*

The implants were manufactured in a metal mold with a 3.0 mm inner diameter and two punches (superior and inferior), warmed and kept at a stable temperature of 180 °C. The mold created by the inferior punch had its cavity filled in three stratified phases. The first layer was composed of a mixture of polyurethane micro-pellets (40% by volume), microfiber bioglass particles (20 vol%), and NaCl (40 vol%); the second, a mixture of polyurethane micro-pellets (85 vol%) and microfiber bioglass (15 vol%); and the third layer was composed entirely of polyurethane

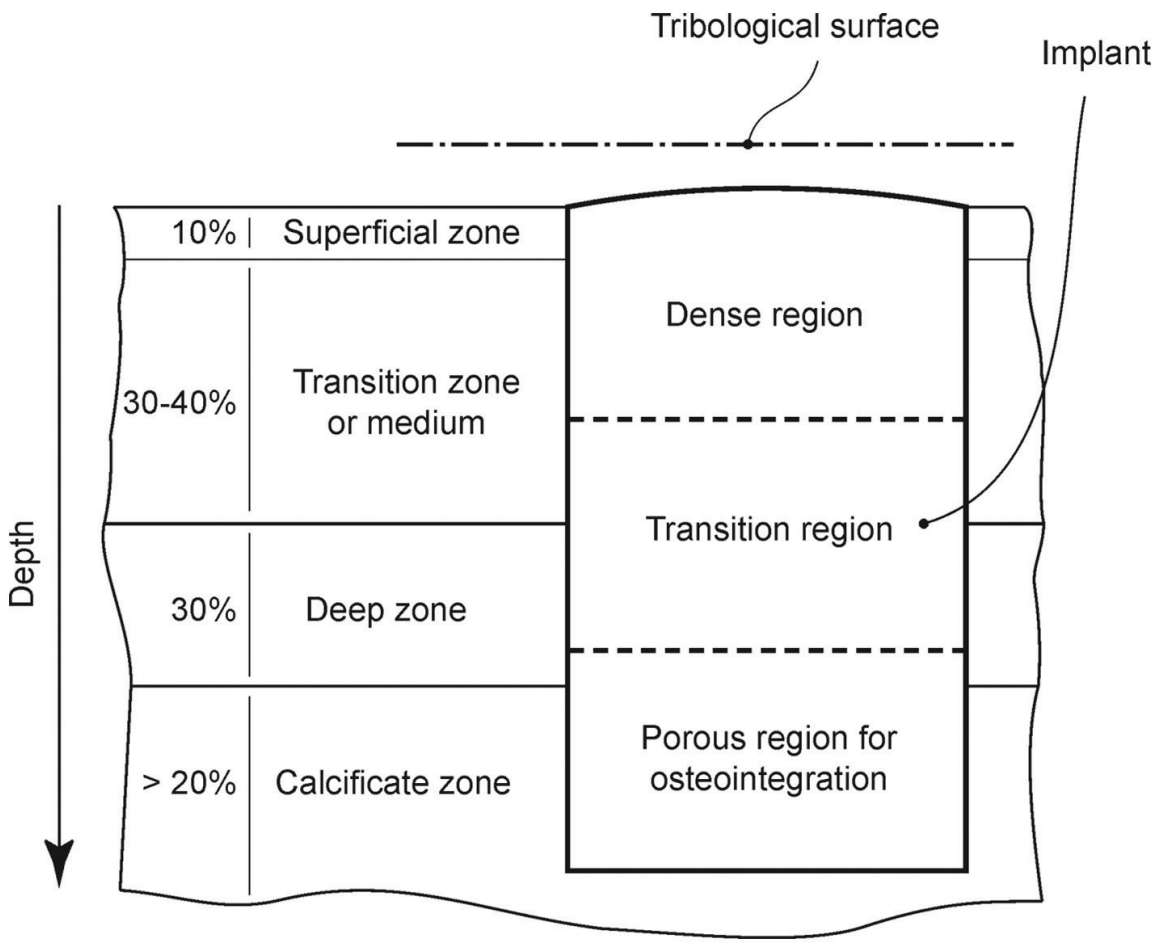

Figure 2. Conceptualization of the specimen in functional gradient.

micro-pellets. After being filled, the mold was closed with a punch and heated for thirty seconds. Subsequently, an uniaxial pressure of 350 MPa was applied for one minute, followed cooling under pressure with circulating water to achieve temperatures of between 40 °C and 50 °C. The samples were radiosterilized with a CO-60 Panoramic dose of 25 kGy and sealed until the time of surgery.

2.4. *Determination of kinetic friction coefficient*

The kinetic friction coefficients of cartilage surfaces against polyurethane, silicone, and glass were experimentally determined. 5 mm-diameter cartilage samples from cow hip joints, a normal force of 10 N, and a displacement velocity of 5 mm/s were employed over a test distance of 10 mm in a saline bath environment

2.5. *Scanning Electron Microscopy (SEM)*

Three samples were selected for SEM analyses. Cuts of thickness ranging from 20 µm to 22 µm underwent SEM analysis after fixation, demineralization, dehydration, diaphanization, and insertion into paraffin. SEM photomicrographs were taken using the Oxford LEO (Model 440) detector operating with an electron beam of 20 kV. The samples were coated with 10 nm of gold in a BAL-TEC MED 020 and kept in desiccators until the time of analysis using standard for co-calibration beam of 20 kV, focal length of 25 mm, 30% dead time, current of 2.82 A and I probe of 950 pA. Mapping was obtained with 20 frames and line-scan with 3000 frames.

2.6. *Atomic Force Microscopy (AFM)*

The microscope was operated in intermittent contact mode using a silicon needle with a spring constant of 70 n/ma and a frequency of 330,000 Hz. This test is justified by the analysis of micro-tribological surface of the polyurethane (merger, union, pores, roughness, etc.) and the osteointegration surface (porosity). This test was performed in two samples (n = 2).

2.7. *Evaluation of the materials' biocompatibility and cytotoxicity*

Vero cells were used from an established fibroblast cell line originating from the kidney of the African green monkey (*Cercopithecus aethiops*) and obtained by the Adolfo Lutz Institute (Sao Paulo, SP, Brazil). The cells were maintained in Ham's F-10 medium supplemented with 10% fetal bovine serum. *In vitro* tests were performed at the Laboratory of Biomaterials in Orthopedics (Labimo), State University of Campinas – Unicamp.

The biomaterials were tested in accordance with current national standards[16] using Vero cells, as recommended by ASTM F813-83 standard[17] to verify cytotoxicity.

Indirect Cytotoxicity – Extracts of 45S5 blown fiber materials and polyurethane were obtained by incubation in Ham F-12 medium with 10% FCS at 37 °C for 48 hours without agitation, at a rate of 01 g/mL[14]. The medium was then collected, allowing the evaluation of the possible effects of the substances released by the different materials that could be present. As a positive control, a solution of phenol of 1% was used in the culture medium. After obtaining the extracts, they were used for the cultivation of Vero cells. The cells were inoculated at a concentration of 1.0×10^5 cells/mL in 24-well plates in Ham F-12 medium with 10% FCS. After 2 hours of incubation, and enough time for cell adhesion, the culture medium was replaced by the extracts or respective control and cultured for 24 hours. Five fields were randomly chosen for each well and the cells were counted using a direct counting method. Images of these fields were also obtained for photographic documentation.

Direct Cytotoxicity – The evaluation of the *in vitro* cytotoxicity of different materials was performed using the cell viability test and the direct cell counting method.

In vivo studies – The surgical protocol was approved by the Ethics Committee of the Sao Carlos Federal University (UFSCar) (approval number: 031/2010). In this study, we used eight adult male New Zealand rabbits with an average weight of 2.5 kg maintained in the bioterium of the Interunits Post-graduation Program in Bioengineering, School of Engineering of São Carlos, São Carlos, Brazil.

Rabbits in the experimental group (n = 6) received a polyurethane and bioglass microfiber implant with a diameter of 3 mm and a depth of 4 mm in the center of the intercondylar region (trochlear groove). The control group (n = 2) received only the bone defect with a diameter of 3 mm and a depth of 4 mm. The animals were kept in individual 70×70×70 cm cages with a ceramic container for industrial water and food pellets *ad libitum*. The *vivarium* lighting followed a cycle of 12/12 h light/dark. The experimental period was 15, 30 and 90 days.

The knee joint was chosen since it is exposed to high mechanical stress over time and because it presents anatomical features that facilitate the surgical approach and the evaluation of the implants' performance. We selected the region of the femoral groove, and not the region of the femoral condyles, because its easier approach makes it a safe and reproducible surgical procedure. Furthermore, the trochlear region of rabbits is exposed to repeated mechanical stresses during walking in the same manner as the region of the condyles[18].

2.8. *Surgical procedure*

Anesthesia was induced by an intramuscular injection of a 5% ketamine hydrochloride solution at a ratio of 50 mg/kg, combined with a 2% xylazine hydrochloride solution at a ratio of 3 mg/kg. Shaving and assepsy were done at the surgical site with a 10% povidone-iodine solution. The surgical technique used was described by Reiff[18]. The surgical access on the knee is the medial longitudinal, extending from the lower region of the patella towards the tibial tuberosity to expose the patellar tendon.

The incision was made in the central portion of the patellar tendon in the longitudinal direction, extending over its entire length and removing the infrapatellar fat in the caudal direction, with subsequent visualization of the trochlear groove of the knee. The osteochondral defect was made in the central region of the femoral trochlea, using a low speed drill of 3 mm of diameter (Figure 3a). The implant was carefully inserted into the osteochondral defect in such way that the tribological surface was at the same level as bone cartilage (Figure 3b).

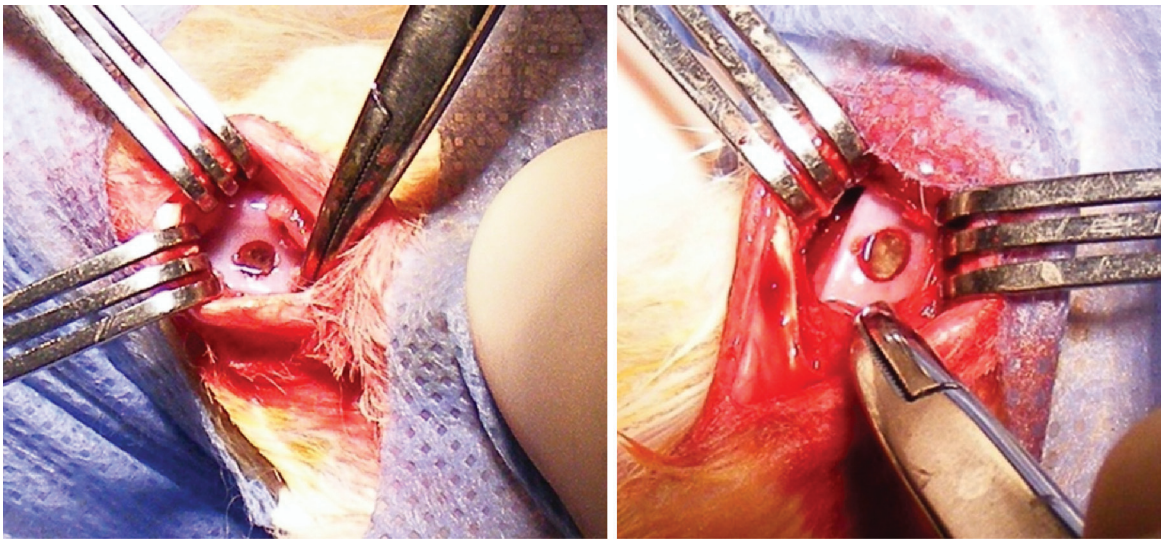

(a) (b)

Figure 3. Surgical procedure: a) bone defect; b) implant placement in osteochondral defect.

For three consecutive days immediately following the surgery, each animal received an intramuscular injection of 1% ketoprofen and a topical application of povidone-iodine on the suture.

After recovery from anesthesia, a normal load on the operated limb was immediately permitted, without any restriction or detention.

The animals were sacrificed 15, 30 or 90 days after surgery. Anesthesia similar to the preoperative anesthesia was used, followed by intravenous injection of 60 mg/kg of potassium chloride.

2.9. *Macroscopic and microscopic analysis*

Macroscopic analysis was used to inspect the external features of the repair of defect. The main characteristics to be analyzed, according to Ribeiro[6], are the surface brightness and consistency of the tissue formed.

The histological samples were collected and fixed in 10% formalin (in 0.1 M phosphate buffer at pH 7.2) for 24 hours. The bones were kept in a decalcification solution until histological sectioning was possible. Samples were then washed in water, dehydrated using increasing concentrations of ethanol, and embedded in paraffin for routine histological techniques. 5mm thick sections were made for different samples. The sections were then stained with hematoxylin and eosin.

3. Results

3.1. *Cytotoxicity tests*

In the studied material, for both direct and indirect cytotoxicity, the quantity of cells is statistically similar to the negative control, and statistically different from the positive control (Figure 4). This indicates no direct or indirect toxicity caused by the sample.

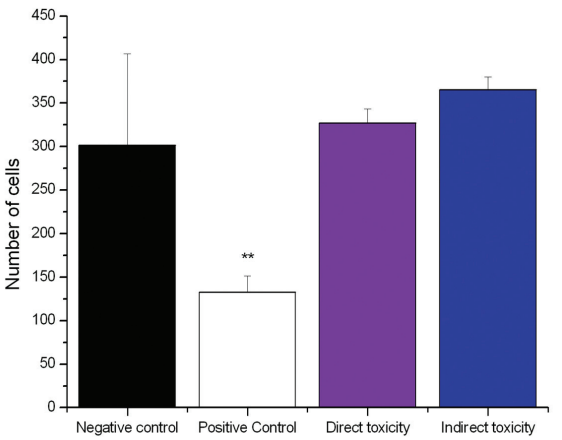

Figure 4. Toxicity of the samples. The positive control of toxicity was significantly different (p = 0.01) from the other samples.

Qualitative analysis showed that the appearance of cells growing under conditions of direct or indirect cytotoxicity is similar to the negative control and different from the positive control (Figure 5).

3.2. *AFM*

The measure of roughness of the tribological side of the specimen, taken using AFM, was 15.74 nm. Figure 6 shows the surface of the melted and subsequently cooled polymer, presenting rounded reliefs and minimal porosity.

3.3. *Determination of kinetic friction coefficient*

A suitable friction between material and the cartilage tissue requires low friction coefficient. In this study, glass exhibited the smallest friction coefficient (see Table 1), and it can be used for calibration. Silicone is a commonly proposed cartilage substitute material. However, polyurethane was

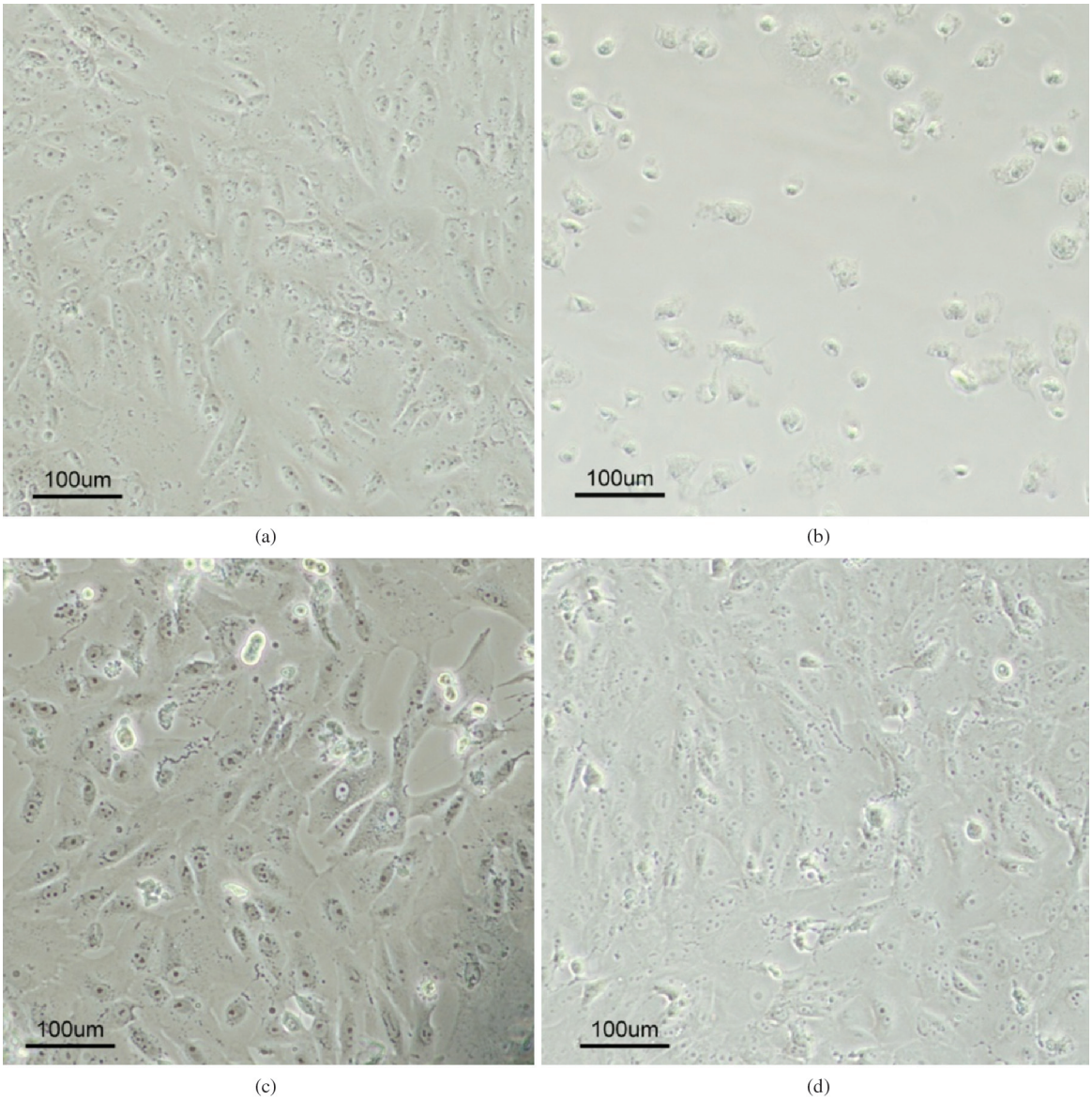

Figure 5. Qualitative morphological assessment of the toxicity of the samples. a) Negative control (non-toxic), b) positive control (toxic); c) direct cytotoxicity, d) indirect cytotoxicity.

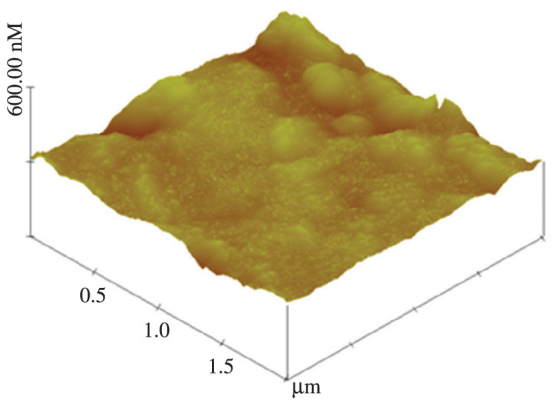

Figure 6. Three-dimensional projection of the tribological surface of the test body.

Table 1. Kinetic friction coefficient of cartilage *versus* materials.

Materials	μ_k
Polyurethane	0,30±0,06
Silicone	0,37±0,09
Glass	0,14±0,06

considered more suitable than silicone for tribologic performance.

3.4. *SEM of the Samples*

The lateral surface of the specimen can be seen in Figure 7a, which shows the differentiation of the proximal, middle and distal tribological surface generated by functional gradient manufacturing. Figure 7c shows the

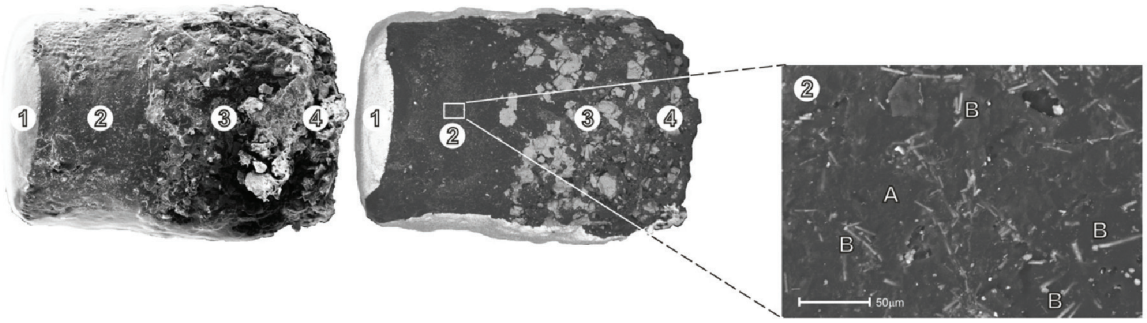

(a) (b) (c)

Figure 7. Implant of bioglass microfiber and polyurethane images performed with SEM: a) surface; b) the same image but with backscattered electrons showing the presence of NaCl in the porosities; c) Section view showing polyurethane matrix (A) and bioglass microfiber 45S5 (B).

substrates used to compose the novel material: polyurethane and microfiber bioglass 45S5. When viewing the sample with the backscattered electron function, the presence of NaCl (evidenced in white) is notable in the porosity remaining after leaching (Figure 7b).

3.5. *Macro and microscopic evaluation – In Vivo Protocol*

The rabbits sacrificed 15 days after implantation showed macroscopic features such as plane surface in the osteochondral defects, growth of fibrocartilaginous tissue, translucent coloration, and a depression-free surface, as shown in Figure 8. Although the rabbits sacrificed after 30 days also showed plane surface, translucent coloration, and a depression-free surface, there was no growth of fibrocartilaginous tissue (Figure 8). Those sacrificed after 90 days presented the following characteristics: presence of plane surface, growth of fibrocartilaginous tissue, transparent color, and no depression on the surface, as shown in Figure 8.

Immediately after the surgical procedure, all rabbits had normal ambulation. The animals showed no signs of infection and the joints remained stable after 15, 30 and 90 days, demonstrating the validity of the experimental method used.

The histological analysis of the control group sacrificed after 90 days showed the presence of bone tissue as well as fibrocartilaginous tissue with chondrocytes and blood vessels (Figure 9).

The SEM photomicrographs of the control group sacrificed after 30 days showed local reabsorption with remodeling of tissues. Figure 10 shows the porous bone formation filling the defect space in the first 15 days of the control group. This structure is similar to the bone trabeculae and was considered biomimetic. Figure 11 shows the occupation of almost the entire porous region by the bone formation after 30 days of implantation, filling the trabeculae with osteoid bone. Figure 12 shows the consolidation of bone formation with dense filling of the porous region and osteon formation 90 days post-experimentation.

4. Discussion

Surgical treatment of chondral and osteochondral injuries that affect load-bearing joints, especially the knee, still represents a challenge for orthopedics due to the characteristics of hyaline articular cartilage, which is devoid of vascularization and has limited potential of cicatrization[6].

Didactically, it is possible to subdivide the tissue regeneration process in three phases: necrosis, inflammation, and repair[19]. Frenkel et al.[20] state that superficial lesions of hyaline cartilage that do not reach the subchondral bone cannot heal normally. Over the time, the progression of the damage produces an irregular and dull macroscopic appearance. However, in injuries extending into the well-vascularized subchondral bone (osteochondral defects), all three stages naturally occur[21]. In the current study, all three phases of regeneration were shown.

At the base of the defect, in the region contacting the subchondral bone, bone formation occurs extending toward the joint. For reasons that are not yet clear, bone tissue formation is often interrupted in the transition zone, allowing the remaining defect to be filled with fibrocartilaginous tissue[7,21]. Histological analysis 15 days after surgery indicated the presence of bone tissue, fibrous tissue with collagen fibers, fibroblasts, blood vessels, and the absence of inflammation. Histological analysis 90 after surgery showed the presence of chondrocytes near the region of the implant, as well as bone tissue and fibrocartilaginous tissue rich in blood vessels.

In the other hand, Huntley et al.[22] state that this new formed tissue that fills the osteochondral defect significantly differs from normal cartilage tissue in its composition and in the arrangement of interior elements. Although chondrocytes synthesize new proteoglycan molecules, they have a lower molecular weight than those found naturally. Similarly, type II collagen fibers have a smaller diameter and more irregular distribution. This arrangement, combined with the fact that there is imperfect integration between the new tissue and the cartilage, favors water permeability. Furthermore, the neoformed fibrocartilaginous tissue has a lower modulus of elasticity than cartilaginous tissue[23,24].

According to Hasegawa et al.[25], the fact that the implants have securely attached since the date of surgery favored

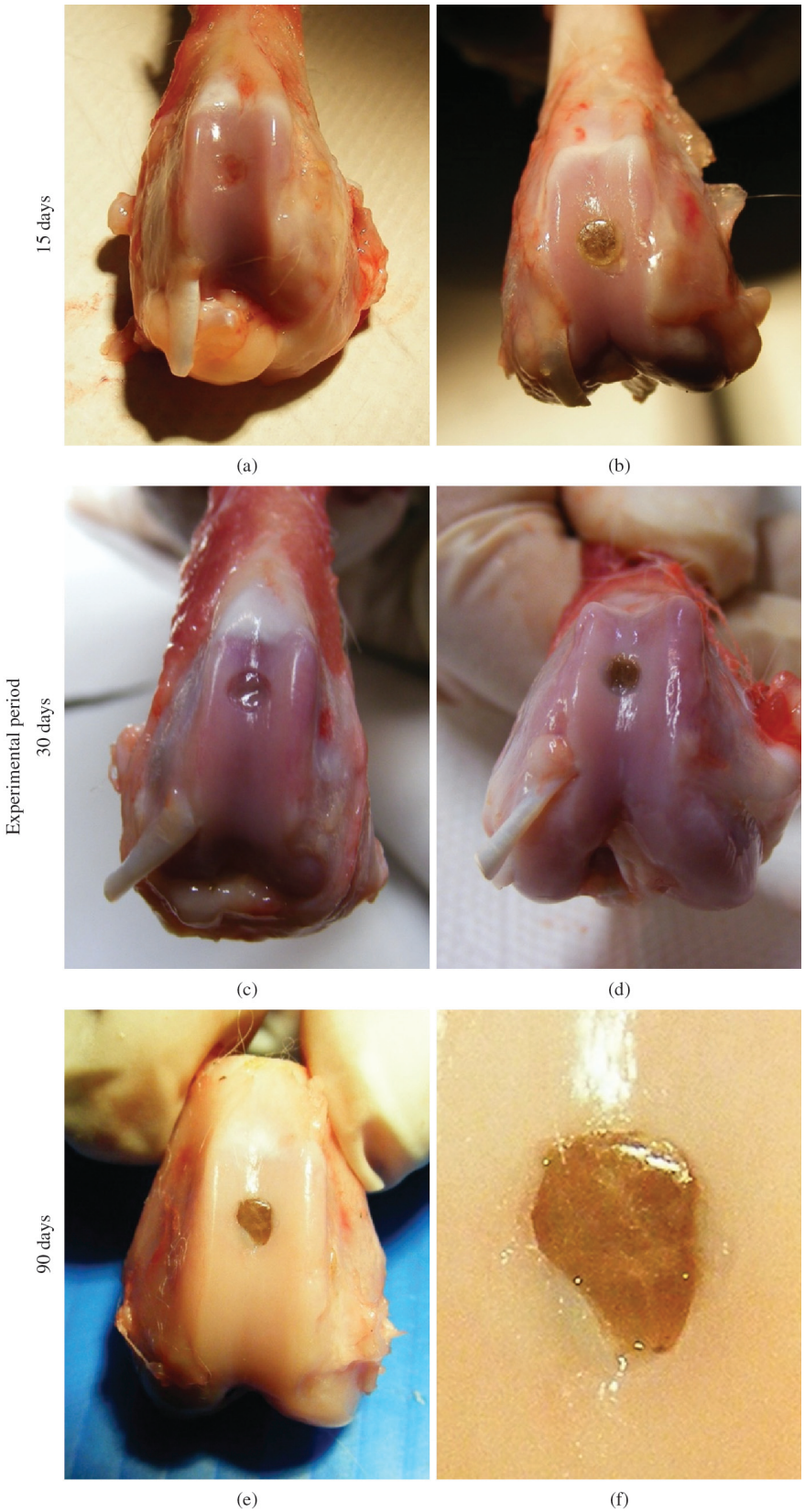

Figure 8. Images of the implant repair, a) control – 15 days; b) implant – 15 days; c) control – 30 days; d) implant – 30 days; e) implant – 90 days; f) implant 90 days with higher magnification.

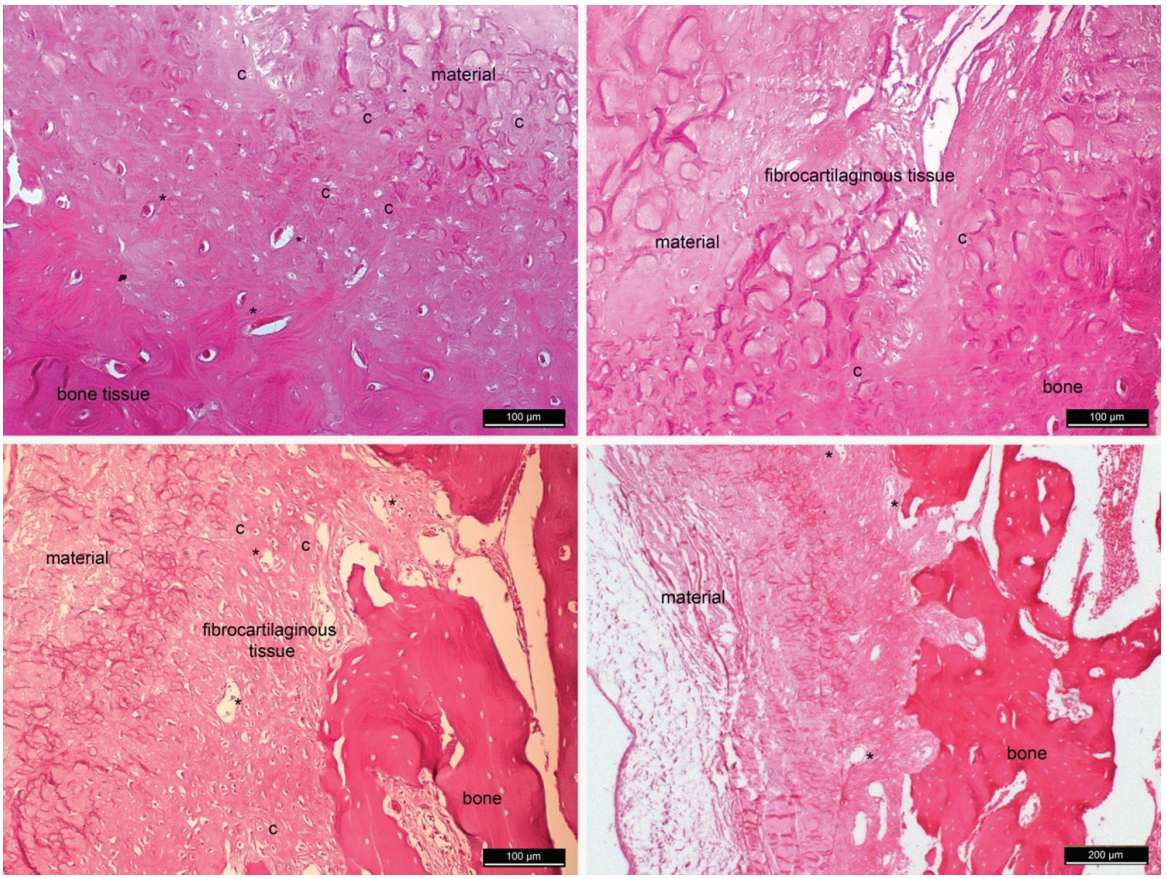

Figure 9. Group 90 days – showing bone tissue, fibrocartilaginous tissue with chondrocytes (c) numerous blood vessels (*) and the material. HE. Increase 100µm.

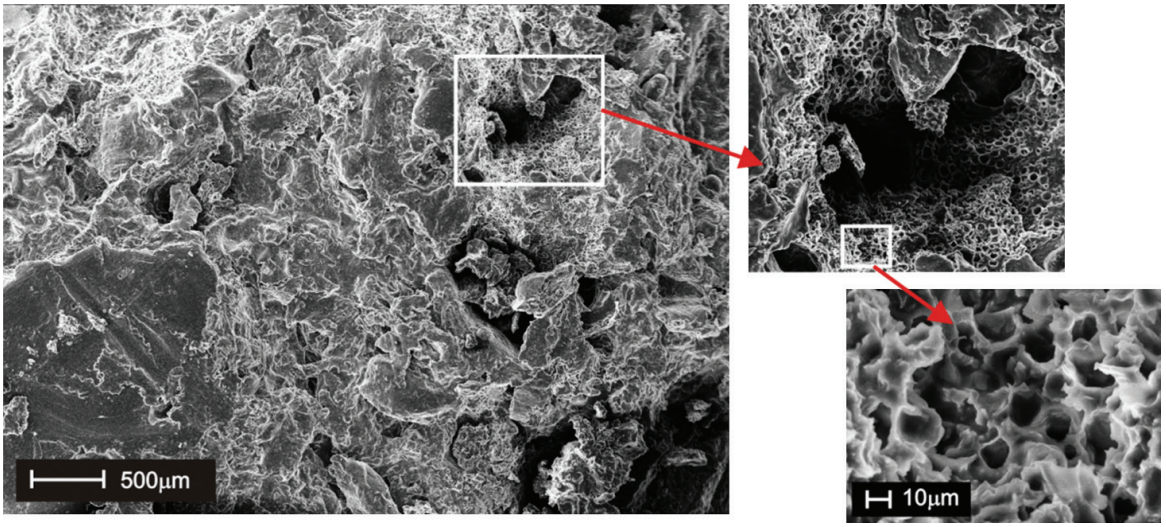

Figure 10. Images of bone formation and space occupation in the porosity with space occupation after the first 15 days under different levels of magnification. The structure is similar to that of the trabeculae bone, which was considered biomimetic.

the formation of bone tissue adjacent to the subchondral bone. Furthermore, they reported the formation of tissue macroscopically similar to cartilage on a part of the implant surface, probably due to the friction between the implant and the patellar surface. Histological examination revealed the newly formed tissue in different period groups.

Biomaterials have contributed significantly to the advance of modern medicine. Driven by collaboration

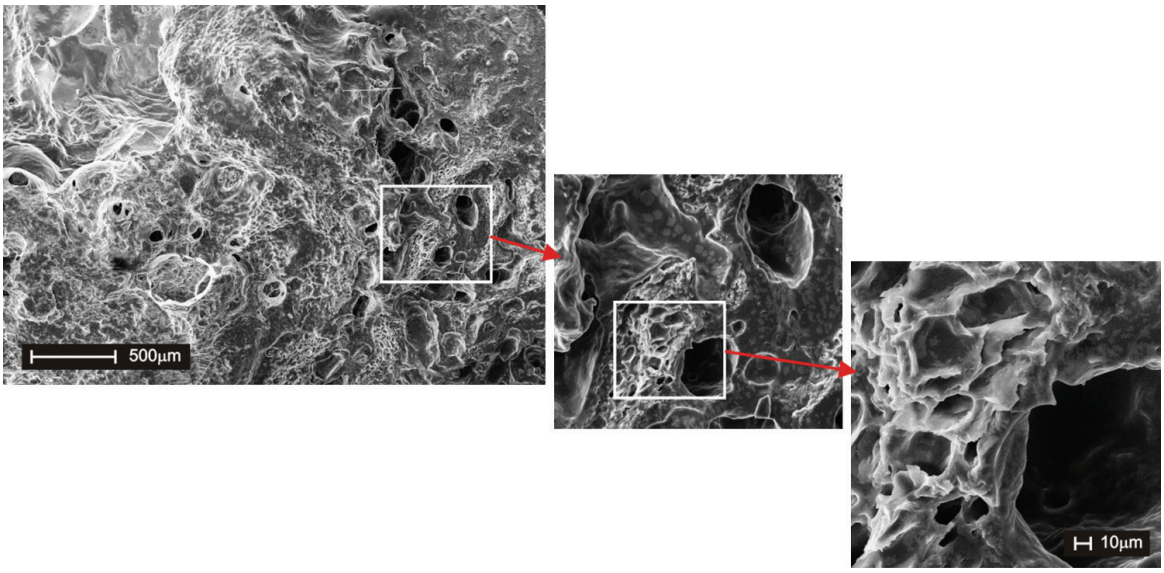

Figure 11. Bone formation occupying almost all the porosity 30 days after implantation under different levels of magnification.

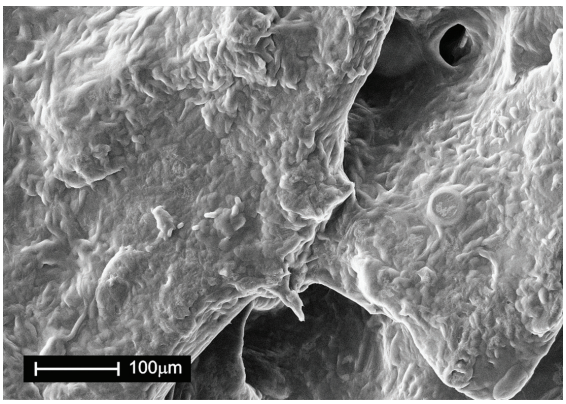

Figure 12. Consolidation of bone formation at 90 days with densified filling of the porous region and osteon formation.

between biomedical engineers, materials scientists, chemists, physicists, biologists and physicians, the science of biomaterials has matured. It has become an area of multidisciplinary research, involving the use of fundamental concepts in the development of materials for clinical practice application. Rapid progress has been achieved in this area, resulting in the synthesis of new ceramic and polymeric biomaterials, the acquisition of knowledge about interactions between biomaterials and biological tissues, the development of artificial organs using cell culture, the advancement of systems for controlled release of drugs, improvement in cardiovascular grafts and devices, miniaturization of prostheses, bone grafts and orthopedic devices.

The characterization of a biomaterial is crucial for determining its performance and consequent definition of the minimum requirements to be met by the industry. In this study, was investigated an essential aspect in developing a biomaterial and its interaction with tissues. Was developed an implant that presents a concept to be applied *in vivo*. The implant maintains the desired mechanical properties and tribological characteristics, and simultaneously ensures good cell adhesion to the bone surface in the intercondylar region of the knee. Once implemented, it is expected to pose a compromise between mechanical properties and biocompatibility. Was described the development of a combination of materials (polyurethane biomaterial compound, microfiber 45S5 bioglass and porous) using manufacturing techniques that are available, reproducible, and technically functional.

With the methodology used in this study, the macroscopic findings in both groups were considered biologically acceptable. The term "biologically acceptable", as defined by Amiel et al.[26], is used to describe repairs with the macroscopic appearance of newly formed tissue similar to fibrocartilage and that are smooth, shiny, firm, and in continuity with the adjacent cartilage. This is a macroscopic criterion of evaluation, and an exact correlation with the histological, biochemical and biomechanical features of the repair cannot be established[6]. Analysis performed 15, 30, and 90 days after surgery demonstrated the characteristics mentioned above in our sample. A SEM photomicrograph taken after 90 days of trial showed the consolidation of bone formation with densified filling of the porous region and osteon formation.

This study is likely to contribute to future research. The biomaterial composed of polyurethane and microfiber bioglass 45S5 described above behaved promisingly due to its biocompatibility, stability, and the absence of inflammatory reaction after 90 days of trial.

5. Conclusion

This study reported on the development and successful validation of a biomaterial composed of polyurethane and bioglass microfiber 45S5 applied as a substitute for articular cartilage, as evidenced by the results of the

in vitro and *in vivo* assays, histological evaluation, SEM and AFM. The biomaterial composed of polyurethane and bioglass microfiber 45S5 showed neither direct nor indirect toxicity in samples and promoted cell growth and spreading, allowing further study using *in vivo* experiments in rabbits. An implant made of polyurethane and bioglass microfiber 45S5 promoted bone formation and complete filling of pores, as well as the presence of chondrocytes. Furthermore, independent of the follow-up time, the implant of polyurethane and bioglass microfiber 45S5 is a promising material because of the following characteristics: biocompatibility after 90 days of experimentation; absence of inflammatory reaction; stability; and the presence of fibroblasts, chondrocytes and osteoid tissue, satisfying the need for cartilage reparation.

Finally, the main advantage is that, due to stability and auto-anchorage to bone and cartilaginous tissues, the implant does not require immobilization, allowing normal weight bearing immediately after surgery.

Acknowledgements

The authors would like to thank Luciana Portal for providing the medical polyurethane and Ted Day from Mo-Sci Corporation for supplying samples of bioglass microfiber. The authors acknowledge the financial support provided by CAPES (Project number PE 0652008 481500/2007-3).

References

1. Rosowski M, Falb M, Tschirschmann M and Lauster R. Initiation of mesenchymal condensation in alginate hollow spheres--a useful model for understanding cartilage repair? *Artificial Organs*. 2006; 30(10):775-784. http://dx.doi.org/10.1111/j.1525-1594.2006.00300.x
2. Bastiaansen-Jenniskens YM, Koevoet W, de Bart AC, van der Linden JC, Zuurmond AM, Weinans H et al. Contribution of collagen network features to functional properties of engineered cartilage. *Osteoarthritis Cartilage*. 2008; 16(3):359-366. http://dx.doi.org/10.1016/j.joca.2007.07.003
3. Peretti GM, Xu JW, Bonassar LJ, Kirchhoff CH, Yaremchuk MJ and Randolph MA. Review of injectable cartilage engineering using fibrin gel in mice and swine models. *Tissue Engineering*. 2006; 12(5):1151-1168. http://dx.doi.org/10.1089/ten.2006.12.1151
4. Beris AE, Lykissas MG, Papageorgiou CD and Georgoulis AD. Advances in articular cartilage repair. *Injury*. 2005; 36(Suppl 4):S14-23. http://dx.doi.org/10.1016/j.injury.2005.10.007
5. Lemos C, Filho JSA, Aymoré IL and Barbosa CSP. Sistema ósteo-articular. In: Brasileiro Filho G, editor. *Bogliolo Patologia*. Rio de Janeiro: Guanabara Koogan; 2000. p. 873-927.
6. Ribeiro JL, Camanho GL and Takita LC. Estudo Macroscópico e histológico de reparos osteocondrais biologicamente aceitáveis. *Acta Ortopédica Brasileira*. 2004; 12(1):16-24. http://dx.doi.org/10.1590/S1413-78522004000100003
7. Buckwalter JA, Einhorn TA and Simon SR, editors. *Orthopaedic basic science*: biology and biomechanics of the musculoskeletal system. Michigan: American Academy of Orthopaedic Surgeons; 2000.
8. Bentley G, Biant LC, Carrington RW, Akmal M, Goldberg A, Williams AM et al. A prospective, randomised comparison of autologous chondrocyte implantation versus mosaicplasty for osteochondral defects in the knee. *The Journal of Bone & Joint Surgery (Br).* 2003; 85(2):223-230. http://dx.doi.org/10.1302/0301-620X.85B2.13543
9. Hunziker EB. Articular cartilage repair: basic science and clinical progress. A review of the current status and prospects. *Osteoarthritis Cartilage.* 2002; 10(6):432-463. http://dx.doi.org/10.1053/joca.2002.0801
10. Guan J, Fujimoto KL, Sacks MS and Wagner WR. Preparation and characterization of highly porous, biodegradable polyurethane scaffolds for soft tissue applications. *Biomaterials*. 2005; 26(18):3961-3971. http://dx.doi.org/10.1016/j.biomaterials.2004.10.018
11. Hench LL, Polak JM, Xynos ID and Buttery LDK. Bioactive materials to control cell cycle. *Material Research Innovations.* 2000; 3(6):313-323. http://dx.doi.org/10.1007/s100190000055
12. Causa F, Netti PA, Ambrosio L, Ciapetti G, Baldini N, Pagani S et al. Poly-epsilon-caprolactone/hydroxyapatite composites for bone regeneration: in vitro characterization and human osteoblast response. *Journal of Biomedical Materials Research - Part A*. 2006; 76(1):151-162. http://dx.doi.org/10.1002/jbm.a.30528
13. Hench LL. Bioceramics. *Journal of the American Ceramic Society*. 1998; 81:1705-1728. http://dx.doi.org/10.1111/j.1151-2916.1998.tb02540.x
14. Rezwan K, Chen QZ, Blaker JJ and Boccaccini AR. Biodegradable and bioactive porous polymer/inorganic composite scaffolds for bone tissue engineering. *Biomaterials*. 2006; 27(18):3413-3431. http://dx.doi.org/10.1016/j.biomaterials.2006.01.039
15. Day RM, Boccaccini AR, Shurey S, Roether JA, Forbes A, Hench LL et al. Assessment of polyglycolic acid mesh and bioactive glass for soft-tissue engineering scaffolds. *Biomaterials*. 2004; 25(27):5857-5866. http://dx.doi.org/10.1016/j.biomaterials.2004.01.043
16. Associação Brasileira de Normas Técnicas – ABNT. *NBR ISO 10993*: avaliação biológica de produtos para saúde. Parte 1: avaliação e ensaio. Rio de Janeiro: ABNT; 1999.
17. American Society for Testing and Materials - ASTM. *F813-07*: standard practice for direct contact cell culture evaluation of materials for medical devices. Pennsylvania: ASTM; 2007.
18. Reiff RBM. *Reparo de defeito osteocondral no joelho de coelhos utilizando centrifugado de medula óssea autóloga*. [Tese]. São Paulo: Universidade de São Paulo; 2010.
19. Mankin HJ. The response of articular cartilage to mechanical injury. *The Journal of Bone & Joint Surgery (Am).* 1982; 64(3):460-466.
20. Frenkel SR, Bradica G, Brekke JH, Goldman SM, Ieska K, Issack P et al. Regeneration of articular cartilage--evaluation of osteochondral defect repair in the rabbit using multiphasic implants. *Osteoarthritis Cartilage.* 2005; 13(9):798-807. http://dx.doi.org/10.1016/j.joca.2005.04.018
21. Mankin HJ. Localization of tritiated thymidine in articular cartilage of rabbits II: Repair in immature cartilage. *The Journal of Bone & Joint Surgery (Am).* 1962; 44(4):688-698.

22. Huntley JS, McBirnie JM, Simpson AH and Hall AC. Cutting-edge design to improve cell viability in osteochondral grafts. *Osteoarthritis Cartilage.* 2005; 13(8):665-671. http://dx.doi.org/10.1016/j.joca.2005.04.007

23. Henderson I, Francisco R, Oakes B and Cameron J. Autologous chondrocyte implantation for treatment of focal chondral defects of the knee--a clinical, arthroscopic, MRI and histologic evaluation at 2 years. *The Knee.* 2005; 12(3):209-216. http://dx.doi.org/10.1016/j.knee.2004.07.002

24. Hattori K, Takakura Y, Ohgushi H, Habata T, Uematsu K and Ikeuchi K. Novel ultrasonic evaluation of tissue-engineered cartilage for large osteochondral defects--non-invasive judgment of tissue-engineered cartilage. *Journal of Orthopaedic Research.* 2005; 23(5):1179-1183. http://dx.doi.org/10.1016/j.orthres.2005.03.014

25. Hasegawa M, Sudo A, Shikinami Y and Uchida A. Biological performance of a three-dimensional fabric as artificial cartilage in the repair of large osteochondral defects in rabbit. *Biomaterials.* 1999; 20(20):1969-1975. http://dx.doi.org/10.1016/S0142-9612(99)00106-4

26. Amiel D, Coutts RD, Abel M, Stewart W, Harwood F and Akeson WH. Rib perichondrial grafts for the repair of full-thickness articular-cartilage defects. A morphological and biochemical study in rabbits. *The Journal of Bone & Joint Surgery (Am).* 1985; 67(6):911-920.